

Parameter optimization and surface integrity aspects in MWCNT-based nano-PMEDM process of Inconel 718

Sinthea Khatun, AKM Nurul Amin, Mamunur Rashid Mashuk, Noshin Tasnim Tuli, Ismat Jerin, M.S. Bashar, Md Jalal Uddin Rumi

Online Publication Date: 30 October 2023

URL: <http://www.jresm.org/archive/resm2023.18ma0530rs.html>

DOI: <http://dx.doi.org/10.17515/resm2023.18ma0530rs>

To cite this article

Khatun S, Amin AKMN, Mashuk MR, Tuli NT, Jerin I, Bashar MS, Rumi Md JU. Parameter optimization and surface integrity aspects in MWCNT-based nano-PMEDM process of Inconel 718. *Res. Eng. Struct. Mater.*, 2024; 10(1): 271-304.

Disclaimer

All the opinions and statements expressed in the papers are on the responsibility of author(s) and are not to be regarded as those of the journal of Research on Engineering Structures and Materials (RESM) organization or related parties. The publishers make no warranty, explicit or implied, or make any representation with respect to the contents of any article will be complete or accurate or up to date. The accuracy of any instructions, equations, or other information should be independently verified. The publisher and related parties shall not be liable for any loss, actions, claims, proceedings, demand or costs or damages whatsoever or howsoever caused arising directly or indirectly in connection with use of the information given in the journal or related means.



Published articles are freely available to users under the terms of Creative Commons Attribution - NonCommercial 4.0 International Public License, as currently displayed at [here](https://creativecommons.org/licenses/by-nc/4.0/) (the "CC BY - NC").

Research Article

Parameter optimization and surface integrity aspects in MWCNT-based nano-PMEDM process of Inconel 718

Sinthea Khatun^{1,a}, AKM Nurul Amin^{1,b}, Mamunur Rashid Mashuk^{1,c}, Noshin Tasnim Tuli^{1,d}, Ismat Jerin^{1,e}, M.S. Bashar^{2,f}, Md Jalal Uddin Rumi^{3,g,*}

¹Dept. of Industrial and Prod. Eng., Military Inst. of Science and Tech., Bangladesh

²Institute of Fuel Research & Development (BCSIR), Bangladesh

³Dept. of Aeronautical Eng., Military Institute of Science and Technology, Bangladesh

Article Info

Article history:

Received 30 May 2023

Accepted 24 Oct 2023

Keywords:

Inconel 718;

NANO-PMEDM;

MWCNT;

Material removal rate

Tool wear rate;

Surface roughness;

Response surface

methodology

Abstract

This study examines the effects of Inconel 718's Nano PMEDM process parameters on Material Removal Rate (MRR), Tool Wear Rate (TWR), Surface Roughness (SR), and the integrity of surface and subsurface layers. It also examines the concentration of MWCNT nanoparticles in distilled water as a dielectric medium. Peak Current, Pulse on Time, and Powder Concentration were input variables in 20 experimental runs utilizing the Central Composite Design (CCD) of Design of Expert (DOE). To create and evaluate empirical models for MRR, TWR, and SR, response surface methodology (RSM) and ANOVA were used. According to the results of the improved RSM, the best responses for MRR, TWR, and SR are 0.012 g/min, 0.001 g/min, and 5.098 μm , respectively. These were accomplished by cutting parameters of 1.5 g/L for powder concentration, 307.967 s for pulse on time, and 19.925 Amps for peak current. GA optimization produced slightly different optimal values for MRR, TWR, and SR: 0.012 g/min, 0.003 g/min, and 5.229 μm , respectively. 20.178 Amps for Peak Current, 398.753 seconds for Pulse on Time, and 3.66 g/L for Powder Concentration were the suggested ideal cutting conditions for GA optimization. In the validation tests, both the GA-predicted outcomes and RSM-optimized values closely matched the experimental results.

© 2024 MIM Research Group. All rights reserved.

1. Introduction

Inconel 718 is a high-tech structural material for crucial industrial applications because of its outstanding corrosion resistance, excellent toughness, and high-yielding strength at extreme temperatures. It has the possibilities for use in an extensive range of fields, such as developing nuclear reactors, jet engines, and turbine engines [1]. Furthermore, it is utilized in producing components for gas turbines, related components for rocket and aircraft engines (such as compressor blades), and spacecraft. Additionally, Inconel 718 has a diversity of products for the gas, oil, and chemical industries [2].

Because it can be strain-hardened while keeping a lessened thermal conductivity, Inconel 718 is a material considered difficult to machine. This is because it maintains both of these properties up to high temperatures. That's the case despite the material's significant advantages [3]. The poor thermal conductivity of the material leads to high cutting temperatures during the machining process. The thermal consequences are apparent because of the high cutting temperature and the material's poor thermal conductivity. Moreover, the material undergoes a chemical reaction that affects the cutting force and the

*Corresponding author: jalal.rumi@ae.mist.ac.bd

^a orcid.org/0009-0007-2943-1292; ^b orcid.org/0000-0002-5259-5072; ^c orcid.org/0009-0000-3101-8471;

^d orcid.org/0009-0007-2750-6385; ^e orcid.org/0000-0003-0369-4952; ^f orcid.org/0000-0001-9793-4348;

^g orcid.org/0000-0002-6404-4438

DOI: <http://dx.doi.org/10.17515/resm2023.18ma0530rs>

Res. Eng. Struct. Mat. Vol. 10 Iss. 1 (2024) 271-304

surface finish achieved after machining [4]. The tools get worn out faster because of the work's tendency to toughen. Because it includes hard abrasive carbide particles, excessive tool wear occurs during machining [5]. Because of all the factors covered earlier, the machining of Inconel 718 should be accomplished at minimal cutting speeds. This significantly decreases the effectiveness of the operation and pushes up the cost of production [2].

To get around the issues of poor machinability of Inconel 718, a significant number of alternative techniques and procedures, including the application of rotary tools, EDM aided by the shuddering of ultrasonic, collective electrodes, and lastly, the combination of supplements in the dielectric fluid have been tried. Introducing powder particles to the dielectric fluid of the EDM process is also referred to as PMEDM (Powder Mixed Electric Discharge Machining) process. Due to the artificial residues, the dielectric resistance was broken down more efficiently, and the machined areas had an excellent finish on the surface [6]. On the converse side, the drawbacks of electro-discharge machining are its relatively leisurely machining process and a moderate material removal rate (MRR). However, to overcome the high cost of conventional machining of difficult-to-machine materials EDM is considered an option. The new concepts of PMEDM are being looked at as potential solutions to the shortcomings of conventional EDM [7]. PMEDM improves overall machining performance over conventional EDM by adding powder particles of the right size and concentration to the dielectric medium [8]. Including metallic powder creates more intense sparks, improving the MRR. At the same time, the spark is dispersed on the powder particles, and as a result, the spark's discharge density reduces. This leads to a reduced number of cracks, holes, and gaps on the surface of the workpiece which has been constructed [9].

EDM efficiency was assessed using carbon Nanotube powders, graphite powders, and nano-sized titanium dioxide powders. The low-energy EDM technique with the CNT (Carbon Nanotube) mixed dielectric also worked. High thermal conductivity, low specific gravity, and superior mechanical and electrical qualities are all characteristics of CNTs. Single-walled carbon nanotubes (SWCNTs) and multi-walled carbon nanotubes (MWCNTs) are the two primary subcategories of CNTs. MWCNTs are more chemically and thermally stable than SWCNTs. Additionally, MWCNTs are less likely to develop oxide than SWCNTs and have greater strength and corrosion resistance [8]. A limited number of studies have been conducted on the impact that Multi-Walled Carbon Nano Tubes (MWCNT) combined with water that has been distilled to be used as a dielectric fluid has in the NANO - PMEDM process.

The literature review established that graphite and Nano TiO₂ powders were widely tested to test EDM performance. However, the effect of Multi-Walled Carbon Nano Tubes (MWCNT) mixed in distilled water as a dielectric fluid in the NANO - PMEDM process has received very little research attention.

Jadam et al. [8] investigated the effect of MWCNT powder concentration added to the dielectric media in enhancing the machining performance of Inconel 718. They varied powder concentration (0.5-1 g/L), pulse on-off time (10 μ s), and peak current (2A, 4A, 6A, and 8A) as their input parameter. They found that MWCNT offers less fracture density added dielectric at 0.5 g/l concentration than 1 g/l concentration. High additive concentrations impede effective flushing and effortless debris removal. Crater enlargement results from an increase in peak current. A higher degree of material erosion from the workpiece results from an increase in average crater diameter caused by the rise in peak current. This raises the MRR. However, at MWCNT concentrations of 0.5 g/l compared to 1 g/l, increased MRR is experienced. Another study on the surface roughness and surface topography of Inconel 718 in the PMEDM process, carried out by Ahmed et al.

[10] using the input parameters powder concentration (0,2,4 g/L), Peak current (20 A, 30 A, and 40 A) and Pulse on time (200 μ s, 300 μ s, 400 μ s). As per their investigation, using the highest peak current for surface roughness is not advised. When the peak current increases, the surface roughness also increases. However, the surface roughness will diminish as the pulse duration increases. These studies opened up a direction to investigate the machining performance of the PMEDM process of Inconel 718 under the influence of the parameters mentioned, i.e., powder concentration, peak current, and pulse on time. These are the significant parameters that influence how the process responds.

A total of sixty 3D roughness parameters are developed in order to do a thorough roughness analysis, and they are used to define the majority of surface morphology in terms of certain functions, qualities, or applications. For the EDM Process: The best roughness parameter is S_{PD} , which measures the number of peaks per unit area following the segmentation of a surface into motifs and is calculated at an 8 mm scale. R. Deltombe used Average surface roughness i.e. R_a to measure the surface roughness of the EDM process [11]. The reason for selecting average surface roughness is regardless of the specimens' curing times; the R_a , or average roughness, values stay constant. One explanation for this phenomenon is that two surfaces with different finishing methods can have comparable average roughness (S_a) values but different roughness metrics, such as valley depth, peak curvature, interfacial area ratio, valley void volume, and peak density. This is due to the fact that surface roughness is a multi-dimensional feature and that extra factors are required to shed light on particular texture and profile aspects. Therefore, these characteristics can differ amongst surfaces even while overall roughness and height variations are comparable [12].

The Taguchi method optimizes machining and electrical and mechanical component design throughout most industrial applications. The success of the Taguchi practice is subdued by constant process variables [13]. This method confines optimization to a certain range and level of parameter values, so one may not be aware of a middle-ground combination that could enhance performance. Complex statistical methods like RSM and ANOVA are required to identify all primary relationship characteristics. Thus, the Taguchi technique can be effectively replaced by RSM [14].

RSM is one of the efficient techniques for generating mathematical models from observable data derived from the actual world [15]. This technique is particularly beneficial in circumstances in which the correlation between the inputs and outputs is nonlinear, which tends to make it challenging to figure out the optimal settings utilizing traditional statistical methods such as regression analysis. In addition, one further optimization technique known as the GA works on a population of alternative answers to generate progressively accurate approximations of the right answer that use the Principle of Darwinian (the survival of the fittest) as its cornerstone. GA is distinct from other, more conventional evolutionary algorithms in that it is not focused on locating a single optimal solution but rather on locating a population of optimal results, and it also provides the option to avoid convergent search toward less desirable solutions [16].

As EDM is the process of material removal using electrical sparks and bombardments, the surface roughness generated in the process is not comparable with that achieved in fine machining and grinding followed by polishing, as such the study on the surface roughness generated in the Nano-PMED process was not included in this study, rather an in-depth study on the composition and micro-structural properties of the EDM generated surface and sub surfaces was included in this study. The objective of the study was to identify the aftermath of the EDM bombardment at the plasma temperatures on the generated surface and sub-surfaces. SEM study, EDS analysis, and micro-hardness measurements of the

upper recast layer, the underlining heat-affected zone up to the main base material were included in this study.

Thus, this investigation looks into the machinability of Inconel 718 through the use of the Nano-PMEDM method using MWCNT as the Nano-particles and distilled water as a dielectric medium, and how the effect of MWCNT Nano-powder has on the response parameters – Material removal rate, and tool wear rate. Modeling responses to reduce MRR and TWR are the primary goal of this research. Optimization is conducted using RSM and GA.

2. Materials and Methods

2.1. Workpiece Material

As the entire purpose of the article is to deliver an appropriate configuration of the machine’s settings for the NANO – PMEDM process and this research has taken into consideration a sample of the nickel-based alloy Inconel 718. The alloy’s physical as well as mechanical characteristics and its chemical configurations (expressed as a percentage of total weight) are demonstrated in Tables 1 and 2, respectively.

Table 1. Physical as well as mechanical characteristics of Inconel 718

Property	Property Unit Density	Young’s Modulus	Yield Tensile Strength	Ultimate Tensile Strength	Thermal Conductivity	Specific Heat Capacity	Melting Point
Unit	Kg/m ³	GPa	MPa	MPa (min)	w/m ^{°K}	J/Kg°C	°C
Quantity	8190	200	1100	1375	11.4	435	1260-1336

Table 2. Chemical Configuration of Inconel 718 (wt.%)

Content	Ni	Cr	Si	Cb+Ta	Mo	Ti	Al	Co	Mn	C	Fe
Composition (Wt%)	53.8	18.2	0.09	5.26	2.96	0.94	0.44	0.3	0.064	0.028	Balanced

2.2. Powder Selection and Dielectric Fluid Preparation

2.2.1. Powder Selection

In this particular study, MWCNTs with a purity of at least 95% and a diameter of no more than 100 nm were employed, though the total length of the diameter was significantly greater than 100 nm [17]. Nano powder composed of multi-walled carbon nanotubes (MWCNT) is an elevated material that has the appearance of a cylinder and is comprised of numerous layers of carbon sheets that have been rolled up. The presence of several layers of graphene in MWCNTs and Double-walled carbon nanotubes (DWCNT) gives these nanotubes greater durability than Single-walled carbon nanotubes (SWCNT) do; for which this construction aids in their application in the field of composite material. Because of its superior mechanical, thermal, and electrical properties, it is the material of choice for use in this research. This property makes it appropriate for a broad spectrum of applications, such as energy storage, thermal management, electrical conductivity, etc. The characteristics of the particle are laid forth in Table 3.

The scanning electron microscope (SEM) image of nanoparticles is demonstrated in Fig. 1. On the other hand, the EDX particle count verifies that MWCNT powder particles are the right amount as shown in Fig. 2.

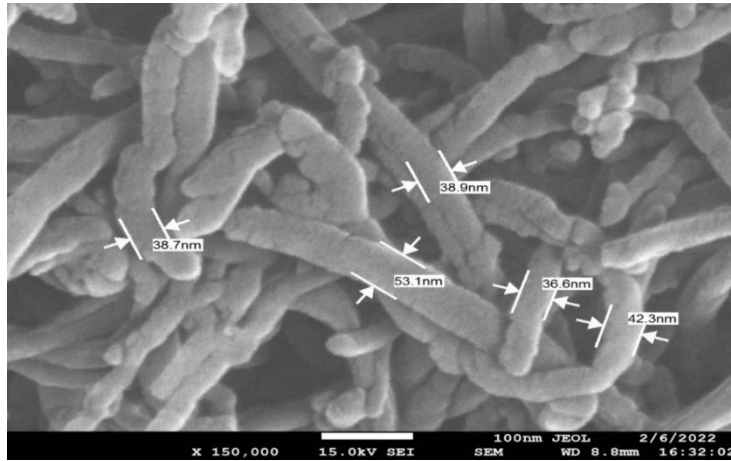


Fig. 1. SEM image of MWCNT powder particle size

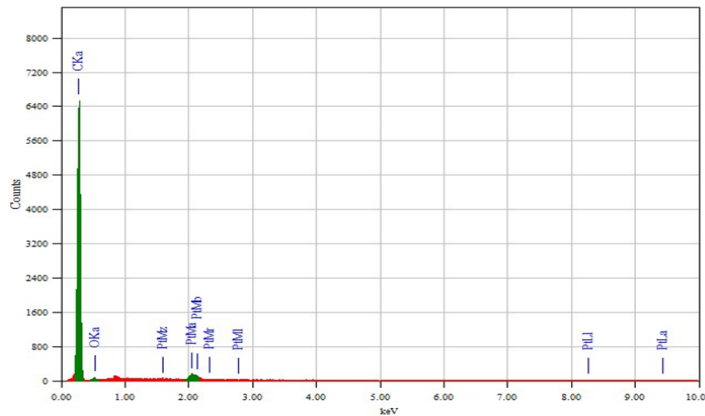


Fig. 2. EDX report for element count

Table 3. Properties of MWCNT

Property	Metallic Impurity	Length	Purity -wt%	Specific Surface Area	Average inner diameter	Number of Walls	Average Outer Diameter
Quantity	<5%	50µm	>95%	350 m ² /g	5 nm	5-15	20-40 nm

2.2.2. Dielectric fluid preparation

Compared to standard dielectric media distilled water provides a lower material removal rate and results in a rough surface finish [18]. However, the incorporation of MWCNT into the distilled used as the dielectric medium causes an appreciable increase in the rate of material removal in contrast to conventional EDM without any additives. The main goal of this study is to judge how well MWCNT nanoparticles coupled with distilled water perform as a dielectric medium in the PMEDM method and assess how well they compare to the

performance of the conventional dielectric fluid. Before starting the testing, the MWCNT nanoparticles were thoroughly mixed with the distilled water using the Sonicator machine. This was to ensure there was no sedimentation during the process. In the process of producing the dielectric fluid depicted in Fig. 3, MWCNT is dissolved.

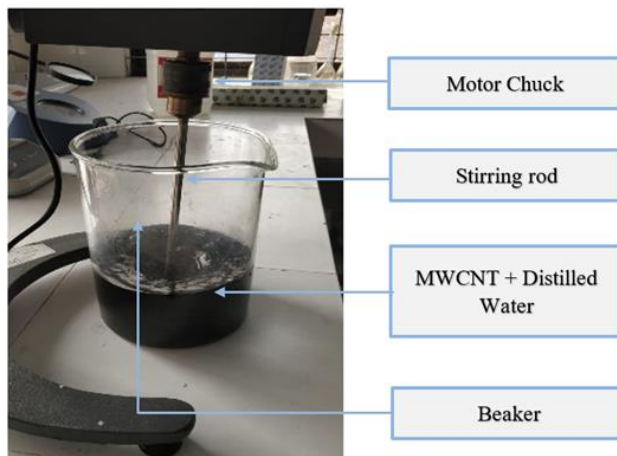


Fig. 3 Preparation of the dielectric fluid (distilled water + MWCNT)

2.3. Cutting Tool

As the experiment will be performed on an electrical discharge machine, the tool must have a high level of electrical conductivity and resistance to arc erosion at the electrode level. Copper and its alloys, graphite, and various other alloys are considered to be suitable to meet these requirements. Copper electrodes have been used in this study, as shown in Fig. 4. The diameter of the tool was maintained constant at 8 mm throughout the entire experiment. Lathe turning and facing were performed before the machining tests.

2.4. EDM Machine

The experiments were conducted on the JS EDM machine model - NCF606N (Fig. 5). A list of the machine's specifications is provided in Table 4. As shown in Fig. 6, the chamber was converted into a small box since the experiments did not require a sizable working space or EDM oil.

Table 4. EDM machine specifications

Parameter	Table dimension	X-axis travel	Y axis travel	Workpiece weight	Ram travel(z)	Max electrode weight	Machine dimension
Unit	mm	mm	mm	Kg	mm	Kg	M
Dimension	700 x 400	450	350	1000	200	120	1.47x 1.15x1.98

Table 5. Input Parameters in Central Composite Design

Name of the Parameter	Unit	Value
Pulse On Time	(μ s)	150-400 μ s
Peak Current	(Amp)	15-40 Amp
Powder Concentration	(g/L)	1.5-5 g/L



Fig. 4. Copper electrode



Fig. 5. EDM Machine

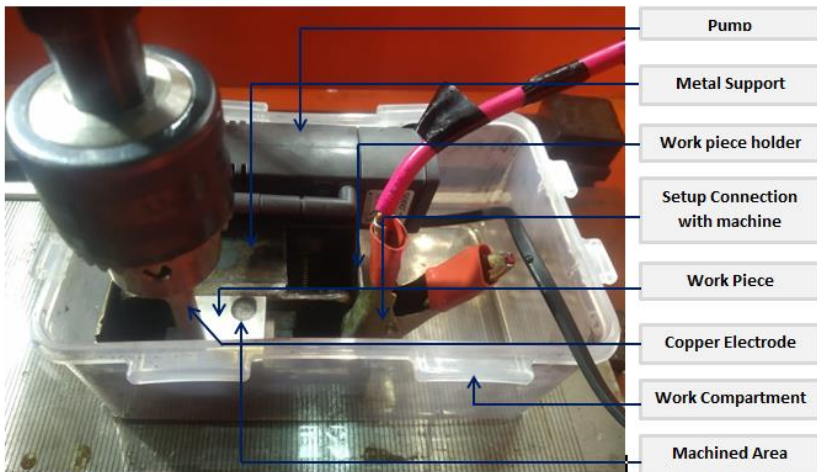


Fig. 6. Experimental setup

2.5. Experiment Design and Parameter Setting

This experiment employs the most influential factors in their appropriate ranges as identified in the prior investigations. Table 5 lists major factors and levels. The study consisted of using RSM analysis based on central composite design (CCD) to properly assess how machining parameters impacted tool wear rate and Surface roughness. The tool diameter of 8 mm and cut depth of 10 mm remain the same throughout the experiment.

3. Result and Analysis

In this study, RSM was used to develop mathematical models of MRR, TWR, and SR as functions of the vital machining factors that included Peak Current (Amp), Pulse On Time (µs), and Powder Concentration (g/L). Necessary computations for the RSM model development were conducted with the help of the Design-Expert software. The tool wear rate as well as the material removal rate was calculated in grams per minute, surface roughness was tested in micrometers as shown in Table 6. A total of 20 different experimental runs were performed under the CCD design of experiments. The influence of MWCNT fine powder was studied varying the Concentration between 1.5–5 g/L. All the electric parameters except peak current (Amp) and Pulse on Time (µs) were constant for each of the runs.

Table 6. Results of experiments on MRR, TWR, and SR in the NANO – PMEDM process

S t u d	R u n	Factor 1	Factor 2	Factor 3	Respon se 1	Predict ed	Respon se 2	Predict ed	Respon se 3	Predict ed
		A: Peak Current	B: Pulse on Time	C: Powder Concentrati on	MRR	MRR	SR	SR	TWR	TWR
		Amp	µs	g/L	g/min	g/min	µm	µm	g/min	g/min
4	1	40	400	1.5	0.02275	0.0226	7.309	7.32	0.00308	0.0032
7	2	15	400	5	0.00779	0.0098	6.216	6.19	0.00109	0.0011
12	3	27.5	485.224	3.25	0.01308	0.0174	8.283	8.41	0.00201	0.0019
14	4	27.5	275	6.19314	0.01291	0.0135	4.4952	4.46	0.00211	0.002
13	5	27.5	275	0.30686	0.01511	0.0155	4.6	4.58	0.00189	0.0018
10	6	48.5224	275	3.25	0.02336	0.0244	6.68	6.6	0.00501	0.0049
11	7	27.5	64.7759	3.25	0.01368	0.0117	4.903	4.73	0.00269	0.0026
9	8	6.47759	275	3.25	0.00264	0.0047	5.43	5.46	0.00085	0.0008
16	9	27.5	275	3.25	0.01343	0.0145	4.58	4.88	0.00191	0.0021
20	10	40	150	1.5	0.01486	0.0193	4.676	4.74	0.0038	0.0039
5	11	15	150	5	0.00516	0.0064	4.361	4.39	0.00119	0.0012
11	12	15	150	1.5	0.00799	0.0076	4.523	4.61	0.00109	0.0012
20	13	27.5	275	3.25	0.01274	0.0145	4.45	4.88	0.00203	0.0021
18	14	27.5	275	3.25	0.01107	0.0145	4.4689	4.88	0.00294	0.0021
19	15	27.5	275	3.25	0.01349	0.0145	5.55	4.88	0.00209	0.0021
17	16	27.5	275	3.25	0.01621	0.0145	5.595	4.88	0.002	0.0021

1	1	27.5	275	3.25	0.0114	0.0145	4.63	4.88	0.0017	0.0021
5	7				7				8	
8	1	40	400	5	0.0249	0.0215	7.453	7.4	0.0032	0.0033
	8				4				9	
6	1	40	150	5	0.0256	0.0181	4.757	4.9	0.0039	0.004
	9				7					
3	2	15	400	1.5	0.0222	0.0109	6.592	6.49	0.0009	0.001
	0				2				1	

3.1. Model Development and Analysis of MRR

RSM was exploited to construct the model employing Design-Expert software, and ANOVA (Analysis of Variance) was suggested to assess the model's adequacy (table-7). The executed fit statistics involved selected responses of MRR found from the experiment presented in Table 6. To compare the models, fit statistics, like p values and F- values are considered.

Table 7. ANOVA of the response MRR

Source	Sum of Squares	df	Mean Square	F-value	p-value	
Model	0.0007	6	0.0001	14.65	< 0.0001	significant
A-Peak Current	0.0005	1	0.0005	59.71	< 0.0001	
B-Pulse on Time	0.0000	1	0.0000	4.95	0.0445	
C-Powder Concentration	4.626E-06	1	4.626E-06	0.5908	0.4558	
AB	0.0000	1	0.0000	1.51	0.2416	
AC	0.0001	1	0.0001	14.60	0.0021	
BC	0.0001	1	0.0001	6.53	0.0240	
Residual	0.0001	13	7.830E-06			
Lack of Fit	0.0001	8	0.0000	3.15	0.1110	not significant
Pure Error	0.0000	5	3.372E-06			
Cor Total	0.0008	19				

The Model F-value of 14.65 implies the 2FI model is significant. There is only a 0.01% chance that an F-value this large could occur due to noise. P-values less than 0.0500 indicate model terms are significant. In this case, A, B, AC, and BC are significant model terms. Values greater than 0.1000 indicate the model terms are not significant. The Lack of Fit F-value of 3.15 implies the Lack of Fit is not significant relative to the pure error. There is an 11.10% chance that a Lack of Fit F-value this large could occur due to noise. Table 8 shows the Predicted R² of 0.4521 is not as close to the Adjusted R² of 0.8117 as one might normally expect; i.e., the difference is more than 0.2. Adeq. Precision measures the signal-to-noise ratio. A ratio greater than 4 is desirable. We found a ratio of 13.103 which indicates an adequate signal.

Table 8. Fit Statistics for MRR

Std. Dev.	0.0028	R ²	0.8711
Mean	0.0145	Adjusted R ²	0.8117
C.V. %	19.26	Predicted R ²	0.4521
		Adeq Precision	13.1033

According to the fit and summary test, a 2FI model was suggested. Equation 1 was confirmed to be the fitting MRR model for Inconel-718 PMEDM:

$$\begin{aligned}
 MRR = & - 0.001723 + 0.000120 * Peak Current + 0.000072 * Pulse on Time - 0.001908 \\
 & * Powder Concentration - 7.76935E-07 * Peak Current * Pulse on Time + 0.000173 * \\
 & Peak Current * Powder Concentration - 0.000012 * Pulse on Time * Powder \\
 & Concentration
 \end{aligned}
 \tag{1}$$

The factor with the coefficient has a ruling impact on the responses. In the case of MRR, powder concentration affects the response more than peak current followed by pulse on time.

3.2. Model Development and Analysis of TWR

The analysis of variance (ANOVA) was conducted to determine whether or not the model that was created by the Design-Expert software was significant by using F-values and p-values of the mode and the mode terms. This was achieved by comparing the results of the ANOVA with the research results of the Design-Expert software. The ANOVA table for this research is illustrated in Table 9.

The fact that the given model is substantial is due to its F-value, which is 50.88. An F-value of this magnitude only has a 0.01% chance of being generated by a noise level of this magnitude, taking into account all of the relevant probabilities. P-values that are lower than 0.0500 are thought to identify that the model terms being considered are significant. Here, the model terms A, B, and A2 are extremely significant. When looking at the data, values that are higher than 0.1000 demonstrate that the model terms do not have statistical significance. The fact that the F-value for lack of fit is only 0.08, which is a relatively low number, lends credence to the hypothesis that it is not statistically significant in comparison to the error.

Table 9. ANOVA for Reduced Quadratic model of TWR

Source	Sum of Squares	df	Mean Square	F-value	p-value	
Model	0.0000	6	3.734E-06	50.88	< 0.0001	significant
A-Peak Current	0.0000	1	0.0000	280.64	< 0.0001	
B-Pulse On Time	5.552E-07	1	5.552E-07	7.56	0.0165	
C-Powder Concentration	6.960E-08	1	6.960E-08	0.9482	0.3480	
AB	1.356E-07	1	1.356E-07	1.85	0.1971	
A ²	8.911E-07	1	8.911E-07	12.14	0.0040	
C ²	9.401E-08	1	9.401E-08	1.28	0.2782	
Residual	9.542E-07	13	7.340E-08			
Lack of Fit	1.094E-07	8	1.367E-08	0.0809	0.9987	not significant
Pure Error	8.448E-07	5	1.690E-07			
Cor Total	0.0000	19				

Based on the fit and summary tests, it was recommended that a quadratic model be used. The results of the analysis of the fitted tool wear rate model for Nano-PMEDM machining of Inconel 718 are presented in (Equation 2) as follows:

$$\begin{aligned}
 TWR = & + 0.000410 + 0.000032 * Peak Current - 1.33805E-06 * Pulse On Time + \\
 & 0.000167 * Powder Concentration - 8.33368E-08 * Peak Current * Pulse On Time + \\
 & 1.61377E-06 * Peak Current^2 - 0.000025 * Powder Concentration^2
 \end{aligned}
 \tag{2}$$

Powder Concentration has the maximum impact on the responses of TWR than Peak Current followed by Pulse On Time as Powder Concentration has the largest coefficient (0.000167) with it.

Table 10 shows that the variance between the predicted and the observed R^2 of 0.9406 as well as the adjusted R^2 of 0.9403 is less than 0.2, indicating that the two values are reasonably comparable to one another. The signal-to-noise ratio is something that Adeq Precision measures. This is preferable to have a ratio that is higher than 4. A sufficient signal can be determined from the ratio of 25.773.

Table 10. Fit statistics

Std. Dev.	0.0003	R^2	0.9592
Mean	0.0023	Adjusted R^2	0.9403
C.V. %	11.87	Predicted R^2	0.9406
		Adeq Precision	25.7732

3.3. Model Development and Analysis of SR

Table 11 provides the results of the ANOVA for the predicted model of SR. It provides both the p-values and the F-values that were formed from the outcomes of the ANOVA for the compact quadratic model of SR eradicating the non-significant terms that had a p-value higher than 0.1. These values were generated from the findings of the ANOVA for the reduced quadratic model of SR. It seems that the model is significant given that it was calculated to have a value of 26.77 for the F-value of the model.

Table 11. ANOVA for the condensed quadratic model

Source	Sum of Squares	df	Mean Square	F-value	p-value	
Model	25.72	7	3.67	26.77	< 0.0001	significant
A-Peak Current	1.55	1	1.55	11.31	0.0056	
B-Pulse On Time	16.34	1	16.34	119.04	< 0.0001	
C-Powder Concentration	0.0175	1	0.0175	0.1277	0.7270	
AB	0.2468	1	0.2468	1.80	0.2048	
A ²	2.37	1	2.37	17.28	0.0013	
B ²	5.12	1	5.12	37.29	< 0.0001	
C ²	0.2333	1	0.2333	1.70	0.2168	
Residual	1.65	12	0.1372			
Lack of Fit	0.1804	7	0.0258	0.0879	0.9970	not significant
Pure Error	1.47	5	0.2933			
Cor Total	27.36	19				

A noise level of this magnitude would only have a 0.01% chance of producing an F-value of this proportion if the noise level were to be increased to this level. P-values for the model terms which are significantly lower than 0.0500 indicate their significance. Within the context of this particular example, the significant model terms are B, A2, and B2. The fact that the F-value for Lack of Fit is 0.09 lends credence to the notion that it does not constitute a statistically significant finding in comparison to the error. Because there is a

99.70% chance that this will be the case, a Lack of Fit F-value of this magnitude could very well be the result of noise.

With this model, one may move more easily through the design space. The fit and summary test indicated that a quadratic model would be appropriate. It was determined that (Equation 3) best represents the surface roughness model that should be used for NANO-PMEDM machining of Inconel-718;

$$SR = +7.37058 - 0.160914 * Peak Current - 0.015037 * Pulse On Time + 0.153404 * Powder Concentration + 0.000112 * Peak Current * Pulse On Time + 0.002597 * Peak Current^2 + 0.000038 * Pulse On Time^2 - 0.041546 * Powder Concentration^2 \tag{3}$$

According to the model, Peak Current has a far greater influence on surface roughness responses than Powder Concentration or iteration, in contrast to TWR. In Contrast, the Pulse on Time has the least amount of influence on the responses when considered an individual parameter.

Table 12 shows that the variation between the predicted and the observed R² value of 0.8961 and the adjusted R² value of 0.9047 is fewer than 0.2, indicating that there is reasonable agreement between the two values. Adeq Precision means signal-to-noise ratio. It is preferable to have a ratio that is higher than 4. A sufficient signal can be inferred from the ratio of 16.838.

Table 12. Fit statistics for SR

Std. Dev.	0.3705	R ²	0.9398
Mean	5.48	Adjusted R ²	0.9047
C.V. %	6.76	Predicted R ²	0.8961
		Adeq Precision	16.8377

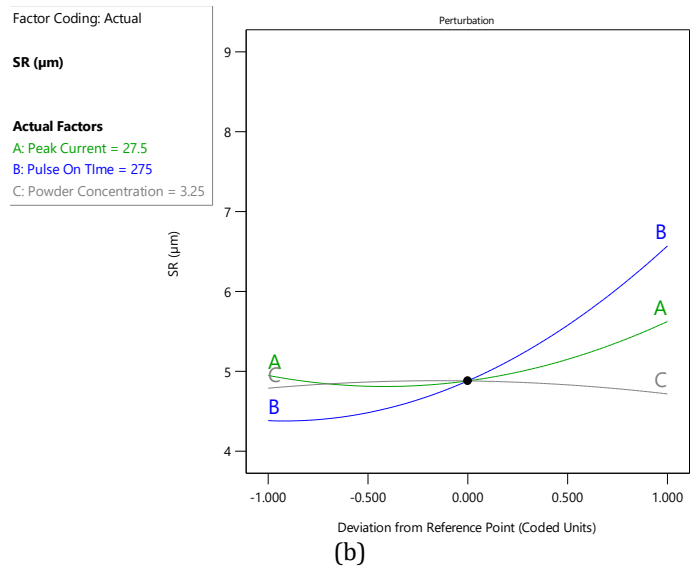
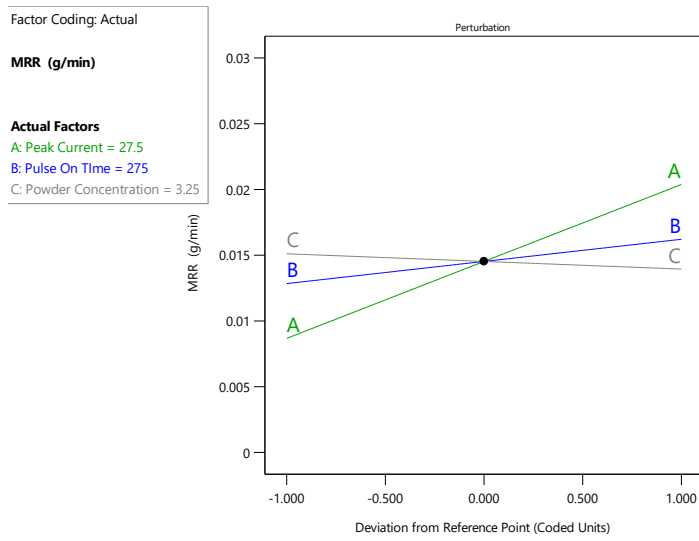
3.4. Perturbation Plot of Machining Characteristics on MRR, TWR, and SR

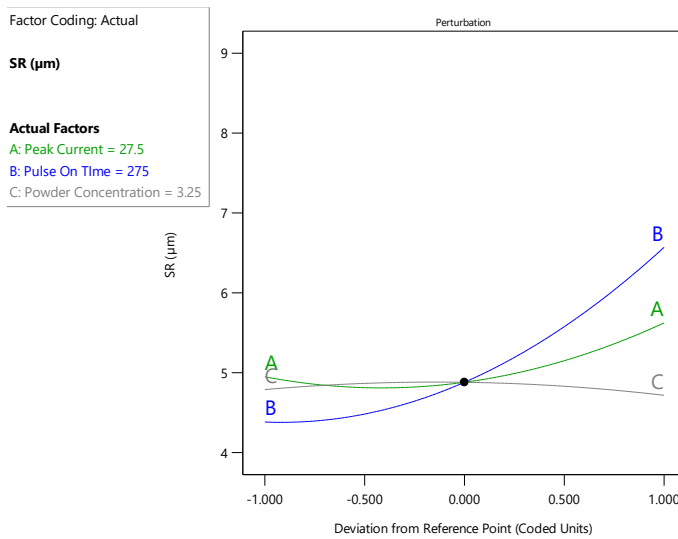
In the significant range, the perturbation plot draws a parallel between the impacts of all three machining parameters and makes comparisons among them. A representation of a perturbation graph of machining parameters on surface roughness and tool wear rate may be found in Fig. 7. All three lines in the picture meet at the same position, which serves as a reference (x = 0.00). The parameters A, B, and C provide a representation of the actual cutting conditions, respectively representing Peak Current (Amp), Pulse On Time (µs), and powder Concentration (g/L). When the reference point (A = 27.5 Amp, B = 275 µs, and C= 3.25 g/L) is moved to the right or left, the graph shows that MRR, TWR, and SR either increase or decrease respectively. The lines drawn on the graph demonstrate that the MRR increases with any movement to the right or approaching +1.00 deviation from the reference point of peak current and pulse on time, however, the MRR marginally reduces with the movement of powder concentration to the right of the intersection point.

This suggests that peak current and powder concentration are critical for MRR. Yet while a drop in powder concentration raises MRR, a drop in peak current drastically lowers MRR. During Peak Current, the TWR value either rises or lowers by a large amount. The TWR decreases at a more gradual rate as both the passage of time and the Powder Concentration increase. In addition, TWR improves if any of those factors move further away from the junction point.

The perturbation plot of SR parameters demonstrates that the aspect that has the most significant effect on surface roughness is the Pulse On Time (B). When factor B (Pulse On Time) is increased from the reference point to a deviation of +1.00, the SR rises quickly.

However, the SR also falls when factor B is decreased, in a manner comparable to that of factor a (Peak Current), but at a more gradual rate. When the Powder Concentration is changed, there is a slight decrease in SR.





(c)

Fig. 7. Perturbation graph of (a) Material Removal Rate (MRR), (b) Tool wear rate (TWR), and (c) Surface roughness (SR)

3.5. 2D & 3D Response Surface Plot

3.5.1. Material Removal Rate (MRR)

Fig. 8 (a) and (b) respectively present the 3D and 2D plots of material removal rate as functions of Peak Current and Pulse on Time. The figures illustrate that peak current has the highest impact on Material Removal Rate. Peak current (at the range 27.5 Amp to 40 Amp) shows the maximum impact on material removal rate when powder concentration is kept constant at 3.25. Interaction between powder concentration and peak current also shows significant improvement in MRR. Increasing Pulse on time, increasing peak current, and decreasing Powder concentration provide the maximum MRR. The combination of the maximum Peak current of 40 Amp, Pulse on time of 400 μs , and minimum powder concentration of 1.5 g/L, an MRR of 0.02 g/min could be achieved. Many other combinations such as Peak current of 37.431 Amp, Pulse on time of 165.162 μs , and powder concentration of 3.865 g/L also give the maximum MRR of 0.020 g/min which indicates increasing peak current and powder concentration while lowering pulse on time can result in high MRR.

Fig. 9 (a, b) presents the (a) 3D and (b) 2D graph illustrating the combined effect of powder concentration and pulse on time on MRR keeping peak current constant at 27.5 A. Varying pulse on time between 150-400 μs and pulse on time between 1.5-5 g/L while maintaining peak current fixed at 27.5 A provides a moderate MRR ranging approximately from 0.012 g/min to 0.018 g/min (Fig. 9 b).

Fig. 10 (a) 3D and (b) 2D graph represents the effect of powder concentration and peak current on MRR while the pulse on time is kept constant at 275 μs . It is clear from Fig. 10 That maximum MRR could be achieved at high peak current and moderate to high powder concentration. According to Fig. 10 b, the red zone for MRR starts at 0.02 g/min which is achieved when the peak current ranges between 35 to 40 Amp and powder concentration

from 3 to 5 g/L. And the maximum MRR achieved by the combination of peak current and powder concentration is 0.0256709 g/min.

Factor Coding: Actual

MRR (g/min)

Design Points:

● Above Surface

○ Below Surface

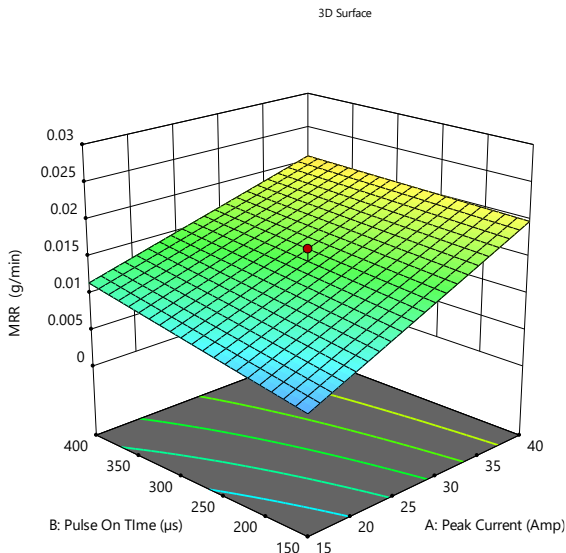
0.00263779  0.0256709

X1 = A

X2 = B

Actual Factor

C = 3.25



(a)

Factor Coding: Actual

MRR (g/min)

● Design Points

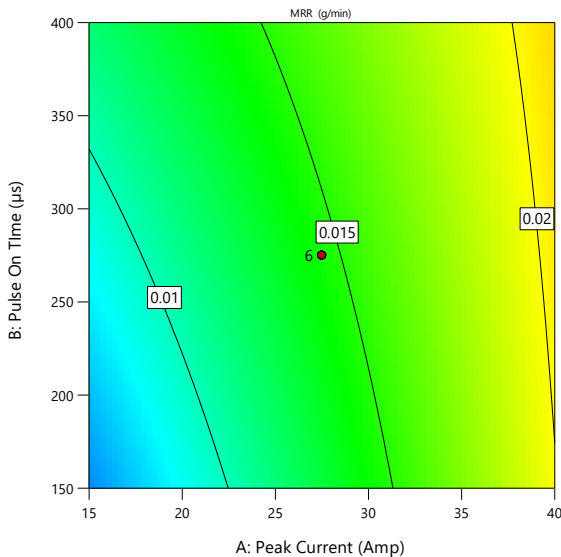
0.00263779  0.0256709

X1 = A

X2 = B

Actual Factor

C = 3.25



(b)

Fig. 8. (a) 3D and (b) 2D plots of material removal rate with effect of Peak Current vs Pulse on Time using MWCNT for Powder Concentration keeping constant at the “3.25 g/L”.

Factor Coding: Actual

MRR (g/min)

Design Points:

● Above Surface

○ Below Surface

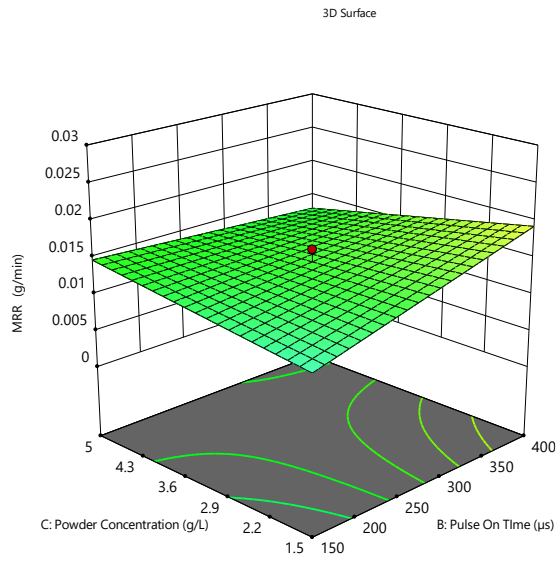
0.00263779  0.0256709

X1 = B

X2 = C

Actual Factor

A = 27.5



Factor Coding: Actual

MRR (g/min)

● Design Points

0.00263779  0.0256709

X1 = B

X2 = C

Actual Factor

A = 27.5

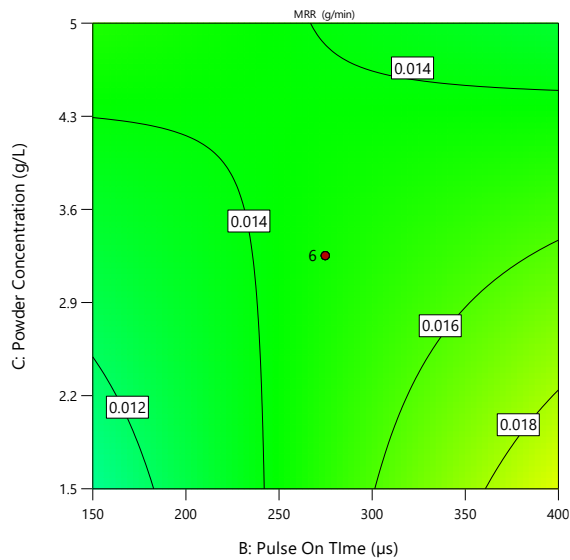


Fig. 9. (a) 3D and (b) 2D plots of material removal rate with effect of Powder Concentration vs Pulse on Time using MWCNT for Peak Current constant at the “27.5 A”.

Factor Coding: Actual

MRR (g/min)

Design Points:

● Above Surface

○ Below Surface

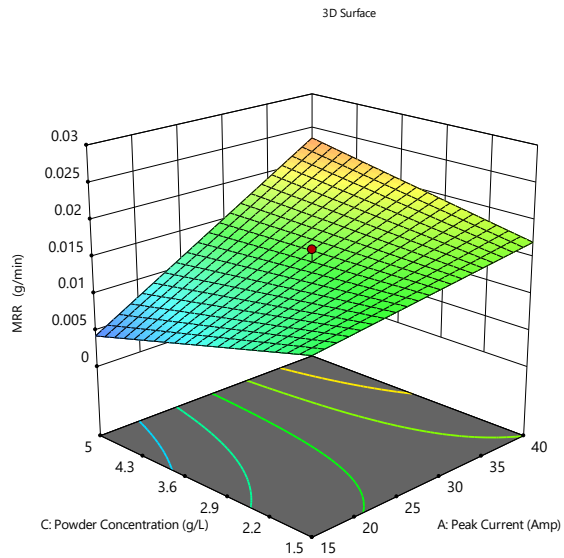
0.00263779 0.0256709

X1 = A

X2 = C

Actual Factor

B = 275



(a)

Factor Coding: Actual

MRR (g/min)

● Design Points

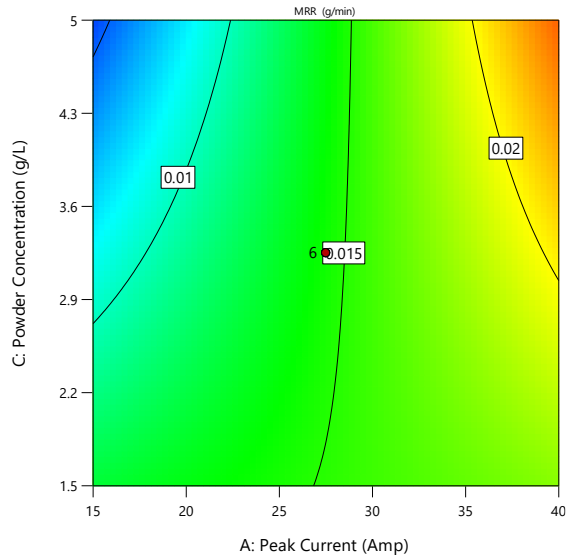
0.00263779 0.0256709

X1 = A

X2 = C

Actual Factor

B = 275



(b)

Fig. 10. (a) 3D and (b) 2D plots of material removal rate with effect of Powder Concentration vs Peak Current using MWCNT for Pulse On Time constant at the “275 μ s”.

3.5.2. Tool Wear Rate (TWR)

The influence of Peak Current and Pulse on Time on the rate of tool wear can be observed in Fig. 11, which displays 3D and 2D responses respectively. It is shown that maintaining the Powder Concentration at 3.25 g/L while reducing the Pulse on Time and increasing the Peak Current can result in the tools getting worn down more quickly. When the Powder Concentration is higher at 4.253 g/L, the Pulse on Time is amplified to 259.229 μ s, and the

Peak Current is increased to 39.361 Amp respectively, the maximum tool wear of 0.004 g/min resulted. This finding is identical to the one that was obtained when the Peak Current was increased to 40 Amp, the Powder Concentration was enlarged to 5 g/L, and the Pulse on Time was reduced to 150 μ s. When the Powder Concentration is held constant, the minimum TWR of 0.001 g/min that is sought can be attained with a lower Peak Current and a Pulse on Time that is higher.

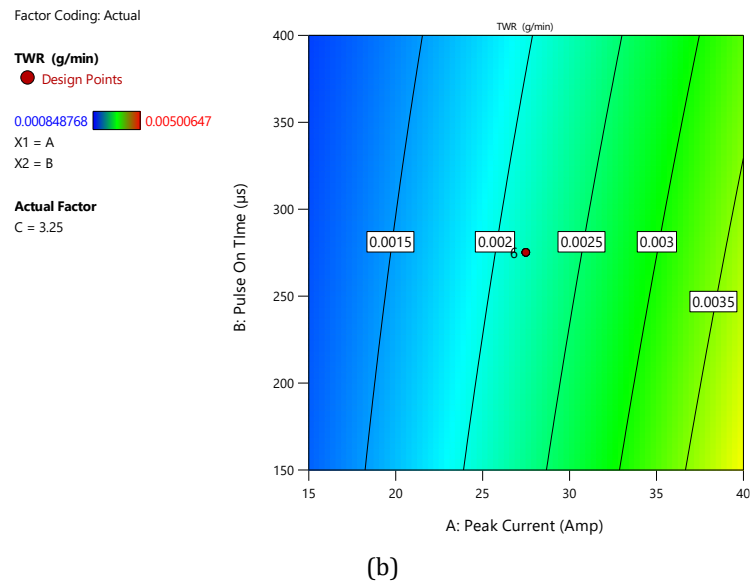
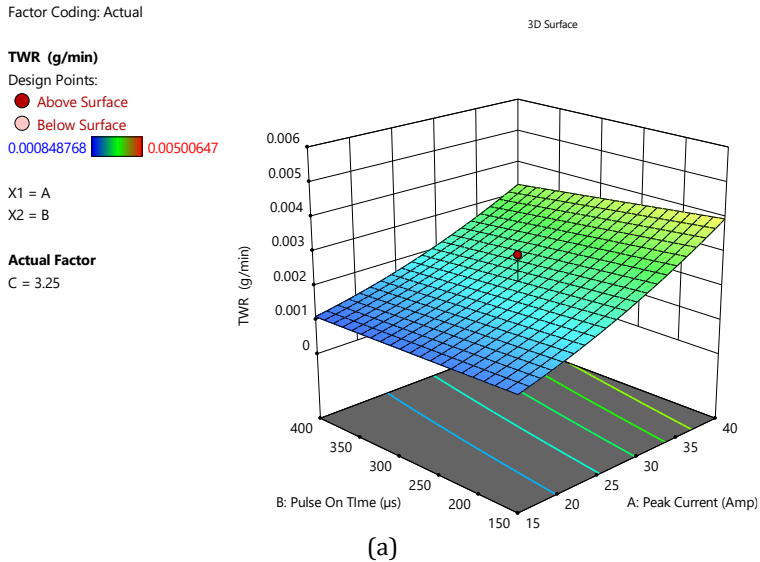
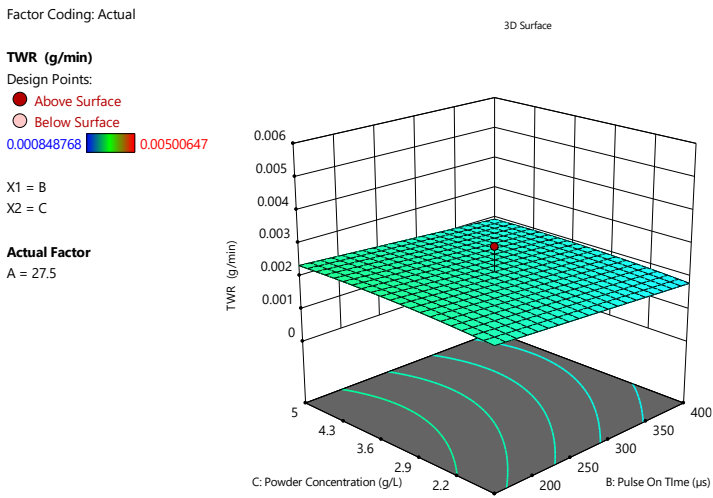


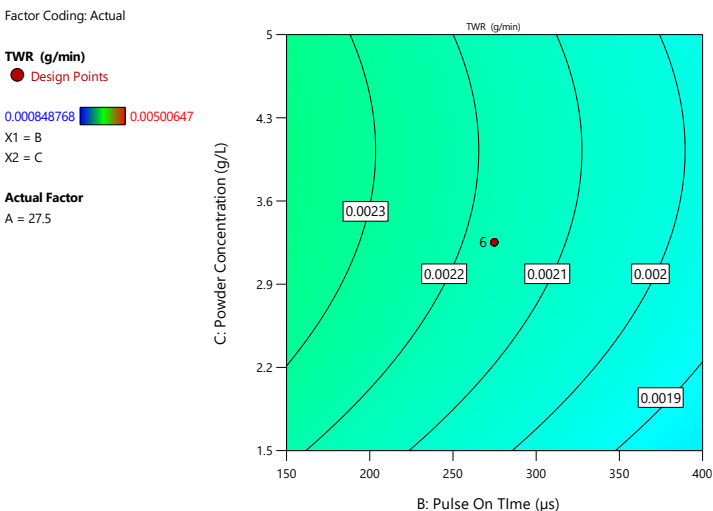
Fig. 11. (a) 3D and (b) 2D plots of Tool wear rate with the effect of Peak Current vs. Pulse on Time using MWCNT for Powder Concentration keeping constant at the “3.25 g/L”.

The combined influence of powder concentration and pulse on time while maintaining the peak current constant at 27.5 A is illustrated at Fig. 12 (a) and (b). The Fig. 12 (a) explains that the combination of high pulse on time and low powder concentrations results in low

tool wear. It is evident from Fig. 12 b that the lowest tool wear that is achieved from this combination is 0.0019 g/min whereas the minimum tool wear possible for the experimental range is 0.000848768. The tool wear rate of 0.0019 g/min is attained from pulse on time ranging between 350 to 400 μ s and powder concentration from 1.5 to 2 g/L.



(a)



(b)

Fig. 12. (a) 3D and (b) 2D plots of tool wear rate with effect of Powder Concentration vs Pulse on Time using MWCNT for Peak Current constant at the “27.5 A”

Fig. 13 a and b illustrates that, if pulse on time is kept constant at a moderate value i.e. 275 μ s and peak current along with powder concentration is varied, then minimum tool wear could be achieved at lowest peak current and average powder concentration. Fig. 13 a proves that minimum tool wear that could be achieved from the combination of powder concentration and peak current is 0.001 g/min while the lowest possible tool wear achievable for this experiment is 0.000848768 g/min. Fig. 13 b represents that the lowest

tool wear blue line which is at 0.0015g/min is achieved at 15 to 25 Amp peak current and 3 to 3.5 g/L powder concentration.

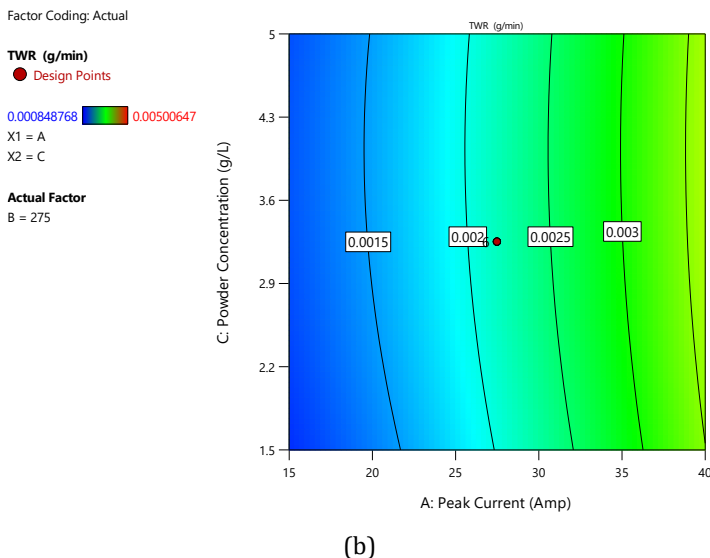
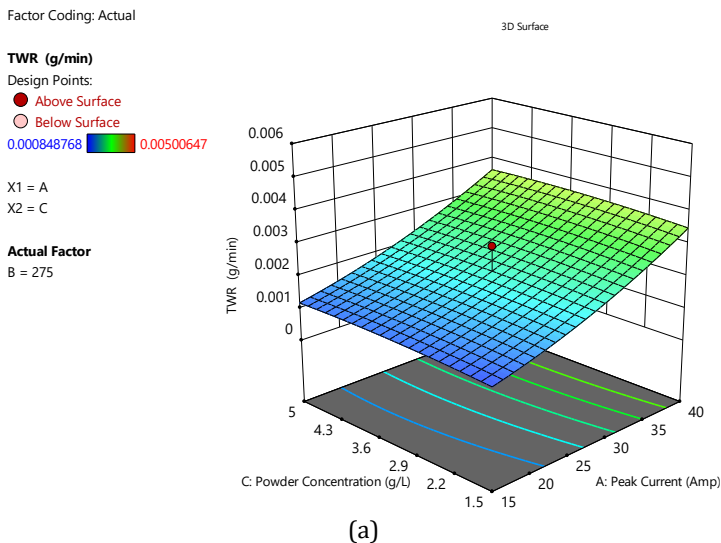
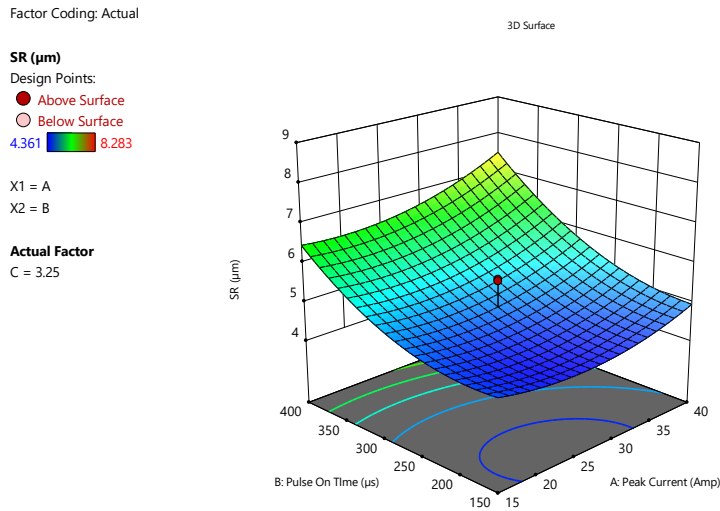


Fig. 13. (a) 3D and (b) 2D plots of tool wear rate with effect of Powder Concentration vs Peak Current using MWCNT for Pulse On Time constant at the “275 μs”

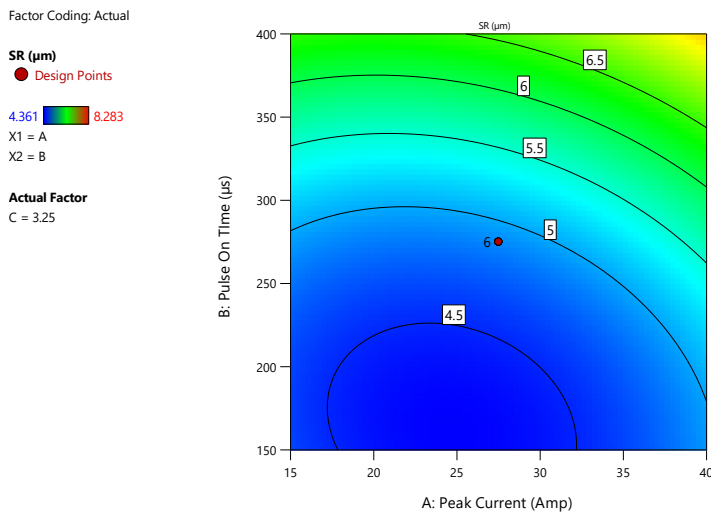
3.5.3. Surface Roughness (SR)

The result of Peak Current and Pulse on Time on Surface roughness illustrating 3D and 2D responses is represented in Fig. 14 (a, b). The figure, it demonstrates that the surface roughness is lower at the range of 15 Amp to 40 Amp of Peak Current and Pulse On Time range of 150 μs to 275μs where the third factor i.e., Powder Concentration is kept steady at 3.25 g/L. However, when Powder Concentration is increased (3.25 g/L - 3.740 g/L), and

the other factors i.e., Peak Current and Pulse on Time 22.622 Amp and 178.172 μs , the experiment showed the minimum surface roughness.



(a)



(b)

Fig. 14. (a) 3D and (b) 2D plots of Surface roughness with effect of Peak Current vs Pulse on Time using MWCNT for Powder Concentration keeping constant at the “3.25 g/L”

The influence of pulse on time and powder concentration on Surface roughness while keeping peak current fixed at 27.5 A is represented at Fig. 15 (a, b). It is illustrated at Fig. 15 (a) that the minimum surface roughness is attainable at low pulse on time and average powder concentration. The 2D graph i.e., the contour graph shows that min SR line where the roughness is 4.5 μm is at the pulse on time range 150 to 250 μs .

Factor Coding: Actual

SR (μm)

Design Points:

● Above Surface

○ Below Surface

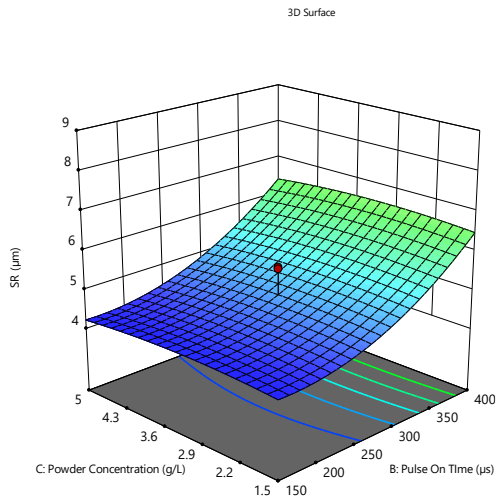
4.361  8.283

X1 = B

X2 = C

Actual Factor

A = 27.5



(a)

Factor Coding: Actual

SR (μm)

● Design Points

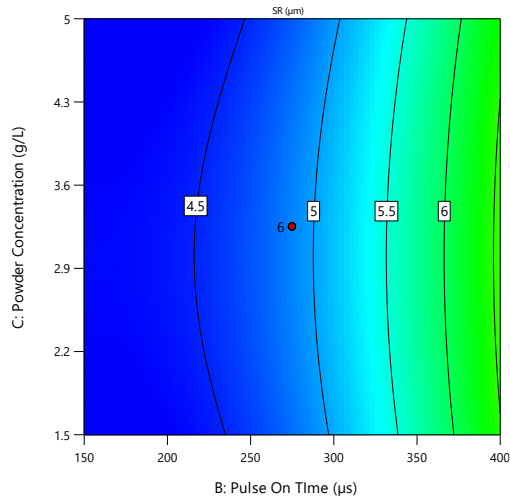
4.361  8.283

X1 = B

X2 = C

Actual Factor

A = 27.5



(b)

Fig. 15. (a) 3D and (b) 2D plots of Surface roughness with effect of Powder Concentration vs Pulse on Time using MWCNT for Peak Current keeping constant at the “27.5 A”

Fig. 16 (a) and (b) is an illustration of how peak current and powder concentration affects surface roughness when pulse on time is kept constant at 275 μs . It is evident from Fig. 16 b that the lowest peak current results in the lowest surface roughness. The minimum surface roughness of 4.361 μm is attained at the lower range of peak current i.e., 15 to 30 Amp. Powder concentration has a little impact on the surface roughness value.

Factor Coding: Actual

SR (μm)

Design Points:

● Above Surface

○ Below Surface

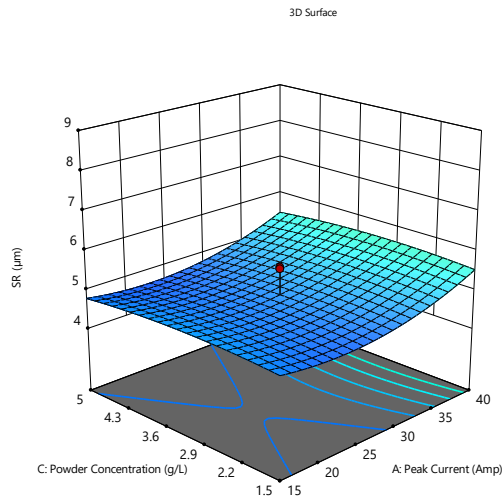
4.361  8.283

X1 = A

X2 = C

Actual Factor

B = 275

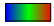


(a)

Factor Coding: Actual

SR (μm)

● Design Points

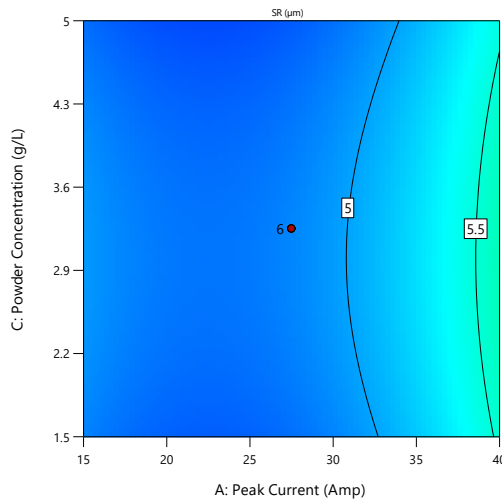
4.361  8.283

X1 = A

X2 = C

Actual Factor

B = 275



(b)

Fig. 16. (a) 3D and (b) 2D plots of Surface roughness with effect of Powder Concentration vs Peak Current using MWCNT for keeping Pulse on Time constant at the “275 μs ”

3.6. Optimization of the Cutting Parameters

This article applied a combined approach of optimization of response variables using the desirability function of RSM and merged models of RSM along with GA to generate optimum values of the desired combinations of output. This approach predicts the best parameter to accurately anticipate response values for every element combination in the experimental zone. The following shows the two optimization methods.

3.6.1. Optimizations of the Response Parameters by Desirability Approach

The desire function approach is quickly becoming among the most important commonly used methods for enhancing multiple response procedures in a wide variety of imposed

scientific and business fields. To construct the most accurate prediction that is even remotely possible, the optimization module will start looking for a combination of factor values that effectively meet all prerequisites for each response and component. This will allow the module to construct the most accurate model possible. This means allowing it to build the most appropriate prediction possible. DFA is a useful method for examining experiments when response needs to be optimized. The optimization of a single response identifies the impact of different input factors on response attractiveness. Prior to anything else, DFA transforms a response into a desirability function that ranges from zero to one. Desirability increases to one when the response variable approaches its aim or goal, and decreases to zero when it is outside of the acceptable range. This technique allows for the identification of the best value at which the tests should be carried out to achieve the lowest level of surface roughness and the reasonable level of tool wear value for the machining configurations that have been clarified. This guarantees that the objective for the factors is set to 'range,' while the reaction is set to 'minimum'. In this work, the target for MRR is to maximize and SR, TWR to minimize as shown at Table 13. As can be seen in Table 14, ten different solutions are ranked, and from those rankings, one solution that is deemed to be the best option is selected.

Table 13. Constraints for optimization of model

Name	Goal	Lower Limit	Upper Limit	Lower Weight	Upper Weight	Importance
A: Peak Current	is in range	15	40	1	1	3
B: Pulse On Time	is in range	150	400	1	1	3
C: Powder Concentration	is in range	1.5	5	1	1	3
MRR	maximize	0.00233779	0.0435882	1	1	5
SR	minimize	4.01	9.123	1	1	4
TWR	minimize	0.00129868	0.00230851	1	1	4

Table 14. Single response optimized solution

Number	Peak Current	Pulse On Time	Powder Concentration	MRR	SR	TWR	Desirability	
1	19.925	307.967	1.500	0.012	5.098	0.001	0.532	Selected
2	19.927	308.092	1.500	0.012	5.100	0.001	0.532	
3	19.912	307.030	1.500	0.012	5.089	0.001	0.532	
4	19.913	307.074	1.500	0.012	5.089	0.001	0.532	
5	19.944	309.309	1.500	0.012	5.112	0.001	0.532	
6	19.960	310.512	1.500	0.012	5.125	0.001	0.532	
7	19.879	304.665	1.500	0.012	5.065	0.001	0.532	
8	19.923	305.727	1.500	0.012	5.075	0.001	0.532	
9	19.867	303.754	1.500	0.012	5.056	0.001	0.532	
10	19.995	313.156	1.500	0.012	5.153	0.001	0.532	

The ideal cutting condition is a Peak Current of 19.925 Amp which indicates Peak Current should be lower, a Pulse on Time of 307.967 μs which is close to the maximum limit of Pulse on Time i.e., 400 μs and a Powder Concentration of 1.5 g/L which is the lower limit

of the range of Powder Concentration. The combination of these parameters results in an MRR of 0.012 g/min, TWR of 0.001 g/min, and SR of 5.098 μm with a desirability of 0.532, which is presented in Fig. 17.

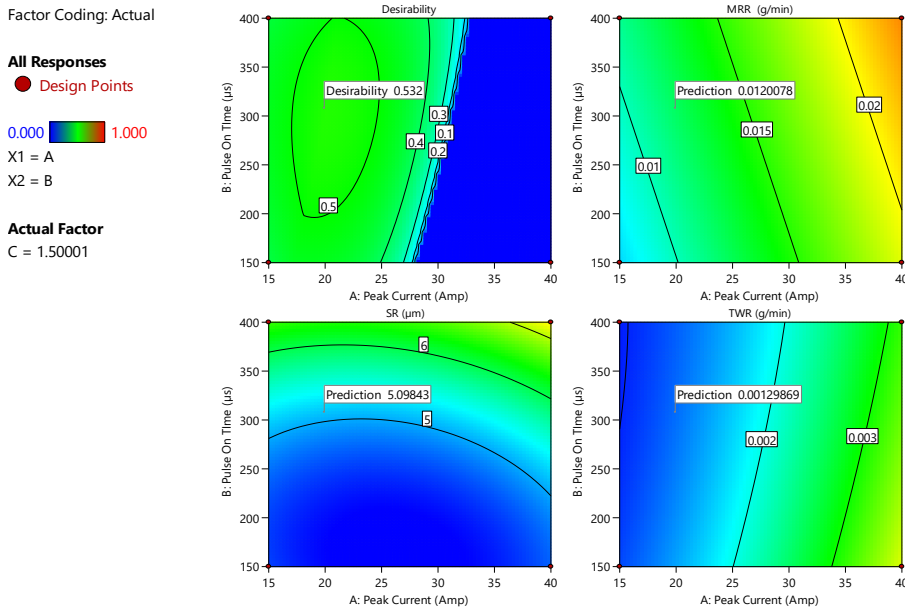


Fig. 17. Contour Graph of optimization

3.6.2. Optimization of The Response Parameters by Genetic Algorithm

Optimization of machining and current parameters in the Nano PMEDM process of INCONEL 718 is what the maximization is trying to achieve. Adjusting parameters with a numerical optimization method is efficient. Maximizing Material Removal rate, Minimizing Surface roughness and Tool wear rate needs a standard mathematical formulation:

Find: A (Peak Current), C (Powder Concentration), B (Pulse on Time)

Maximum: Material Removal Rate (A, B, C),

Objective function; $- 0.001723 + 0.000120 * \text{Peak Current} + 0.000072 * \text{Pulse on Time} - 0.001908 * \text{Powder Concentration} - 7.76935\text{E-}07 * \text{Peak Current} * \text{Pulse on Time} + 0.000173 * \text{Peak Current} * \text{Powder Concentration} - 0.000012 * \text{Pulse on Time} * \text{Powder Concentration}$

Minimize: Tool Wear Rate (A, B, C),

Objective function; $+ 0.000410 + 0.000032 * \text{Peak Current} - 1.33805\text{E-}06 * \text{Pulse on Time} + 0.000167 * \text{Powder Concentration} - 8.33368\text{E-}08 * \text{Peak Current} * \text{Pulse on Time} + 1.61377\text{E-}06 * \text{Peak Current}^2 - 0.000025 * \text{Powder Concentration}^2$

Minimize: Surface roughness (A, B, C)

Objective function; $+7.37058 - 0.160914 * \text{Peak Current} - 0.015037 * \text{Pulse on Time} + 0.153404 * \text{Powder Concentration} + 0.000112 * \text{Peak Current} * \text{Pulse on Time} + 0.002597 * \text{Peak Current}^2 + 0.000038 * \text{Pulse on Time}^2 - 0.041546 * \text{Powder Concentration}^2$

Subject to constrain: $Ra \leq Ra \text{ min}(\mu\text{m})$

Within ranges: $(A_{\text{min}} \leq A \leq A_{\text{max}}), (C_{\text{min}} \leq C \leq C_{\text{max}}), (B_{\text{min}} \leq B \leq B_{\text{max}})$

The variations of parameters to use for cutting in optimization have been selected based on the variable ranges used in the RSM model that was formed. The principles underlying natural selection and genetics are used as the basis for the Genetic Algorithm, which is an iterative search technique used for optimization. It takes its name from the genetic code, which is also its namesake [19]. The fundamentals of GA are simple and involve copying binary strings and then exchanging the binary strings that have been copied with one another. The GA method's primary selling points are the ease with which it can be utilized to perform computations and the speed with which it can do so. The GA solves the optimization problem by using an iterative process that is based on the biological evolution process that takes place in nature (Darwin's theory of survival of the fittest).

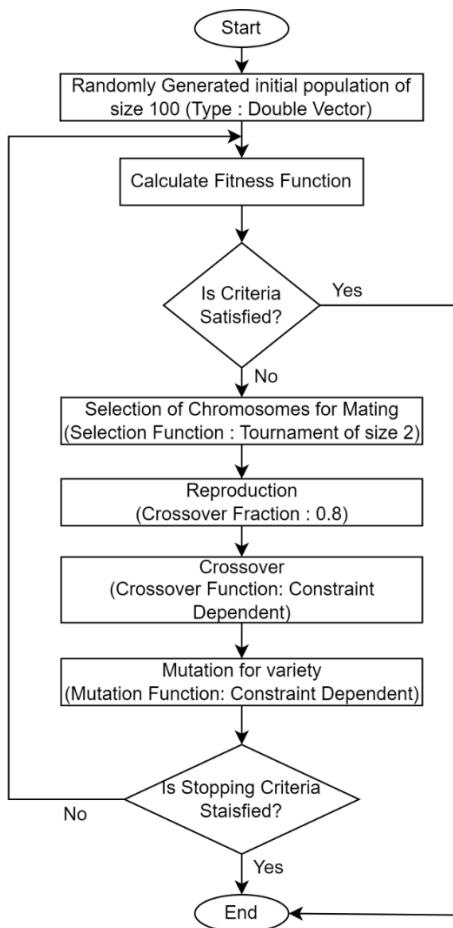


Fig. 18. Processing diagram of optimization utilizing genetic algorithm at matlab

The GA program is developed using MATLAB 2020 Toolbox for GA. The processing diagram for the GA optimization is shown at Fig. 18. GA's important parameters are population size, mutation, generations, etc. Table 15 shows the parameters. The established RSM models for MRR, SR and TWR prediction have served as optimizers for the GA. Based on objective value and constraint violation, the MATLAB GA algorithm picks chromosomes.

The most optimum parameter values used in GA as illustrated in Table 16, are Peak Current of 20.178 Amp, Pulse on Time 398.753 μ s, and powder concentration of 3.66 g/L. GA

predicted optimum results for MRR, SR and TWR are 0.012 g/min, 5.229 μm and 0.003 g/min respectively.

Table 15. Genetic Algorithm parameters

Parameters	Values
Population	100
Selection	Tournament (Size = 2)
Crossover Fraction	0.8
Crossover Function	Constraint dependent
Mutation Function	Constraint dependent
Stopping Criteria	Default
Migration Direction	Forward
Creation Function	Constraint dependent

Table 16. The finest cutting condition found in GA and experimental validation for Inconel 718

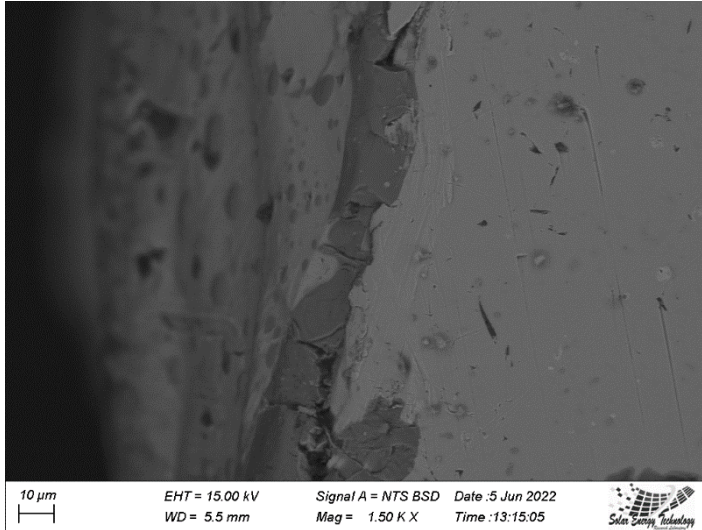
Parameters	Optimized Values
Peak Current, A	20.178
Pulse on Time, B	398.753
Powder Concentration, C	3.66
GA prediction	MRR (g/min) 0.012
GA prediction	SR (μm) 5.229
GA prediction	TWR (g/min) 0.003

4. Surface Characteristics

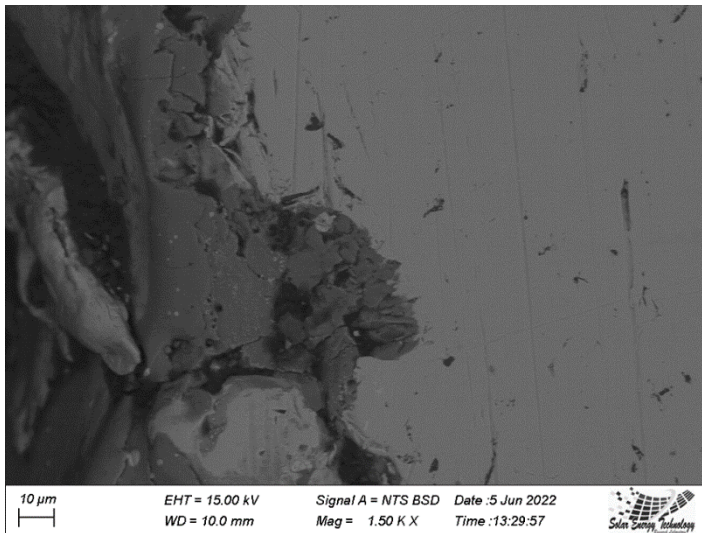
The EDM procedure adversely affects the integrity of the machined surface, as is widely known. During the sparking process in the PMEDM process, the materials in the workpiece and the tool electrode melt due to the high temperature of the spark. This is followed by a speedy re-solidification of the molten materials due to rapid cooling in the machining zone. The composition of the recast layer is of great interest to the researchers as this is the outermost layer to be exposed to the high stresses imposed on the die surfaces. This layer is supposed to contain oxides of the elements of the workpiece and the electrode materials as a result of a chemical reaction with the available oxygen inside the dielectric. The condition and composition of the HAZ are also equally important to know as this layer is going to be exposed to external loads that may be imposed on the part surface. The condition of the underlying base material and its resultant composition is also important to study as it would be a subsequent frontier to overcome the forming stresses applied to die surfaces.

SEM images of the three areas as discussed above for three selected Nano-PMEDM conditions were considered along with the EDS analysis at the three interested zones (Recast layer, HAZ, and Base metal) as indicated in Fig. 19(d). These included the 6th run (Peak Current: 48.5224 Amp, Pulse On Time: 275 μs , Powder Concentration: 3.25 g/L), as illustrated in Fig. 19 (a); 7th run (Peak Current: 27.5 Amp, Pulse On Time: 64.7759 μs , Powder Concentration: 3.25 g/L), as shown in Fig. 19 (b) and the 8th run (Peak Current: 6.47759 Amp, Pulse On Time: 275 s, Powder Concentration: 3.25 g/L) as displayed in Fig. 19 (c). The average recast layer thickness obtained after the sixth, and seventh operations are 18.5 μm and 48.2 μm respectively. The average HAZ thickness followed by the recast layer observed is 16.134 μm and 85.13 μm respectively. No discernible heat-affected zone or recast layer is present at the machined zone of the 8th run. Fig. 19 (a, b, c) makes it clear

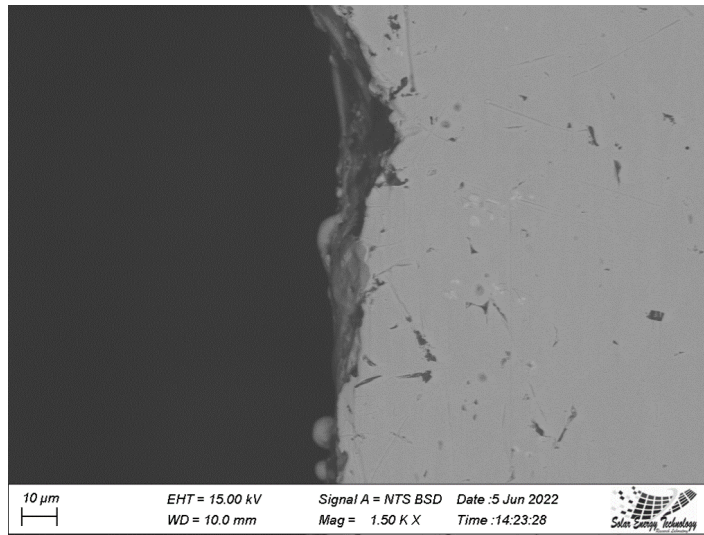
that the recast layer is uneven in thickness and contains craters and debris. The surface of the heat-affected zone has numerous microcracks and craters. Fig. 19 (b) has more craters and unevenness than Fig. 19 (a), as well as a thicker recast layer and HAZ. Peak current and pulse on time are the variables that triggered this alteration. High peak current and pulse-on-time values provide a surface that is more uniform and has fewer craters in comparison.



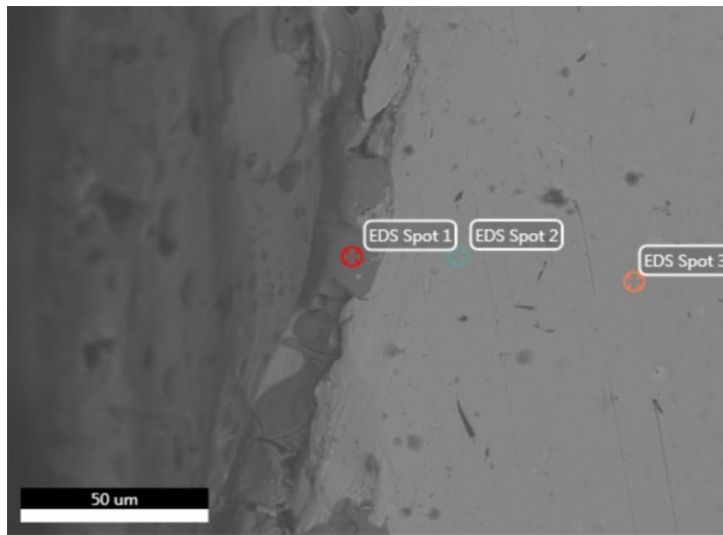
(a)



(b)

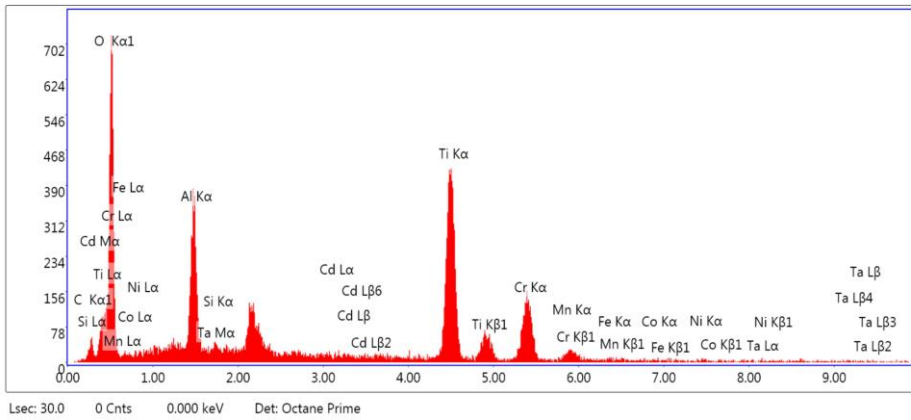


(c)

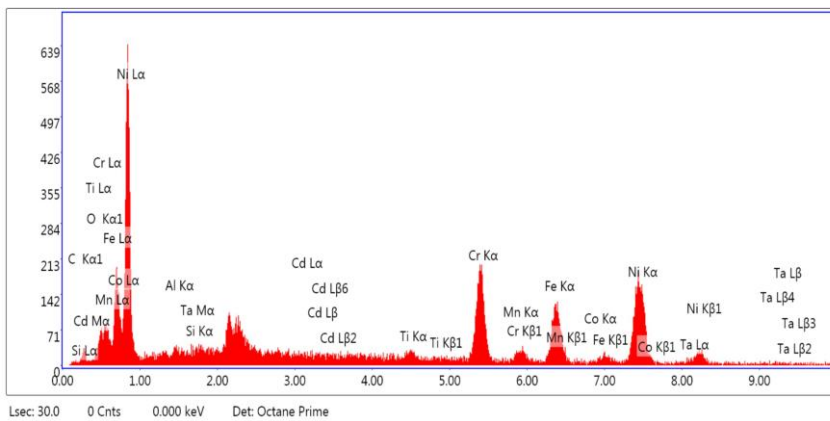


(d)

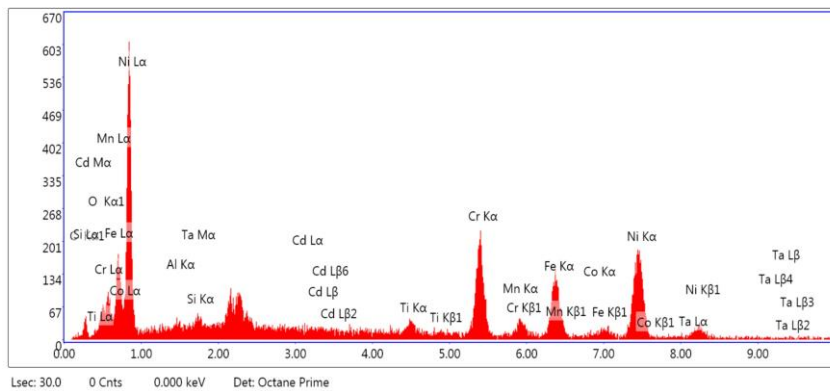
Fig. 19. SEM top view of the machined surface obtained during Nano-PMEDM machining of Inconel 718 under MWCNT for (a) sixth run, (b) seventh run, (c) eighth run, and (d) spots selected for EDS analysis



(a) EDS Spot 1, at the recast layer



(b) EDS Spot 2, at the heat-affected zone



(c) EDS Spot 3, at base metal

Fig. 20. Energy Dispersive Spectrometry (EDS) microanalysis of the machined surface, obtained during Nano-PMEDM machining of Inconel 718 under MWCNT mixed with distilled water dielectric medium for 6th run

To determine the components, present in the three separate zones, three specific spots at the base metal, heat-affected zone, and recast layer were selected (Fig. 19 d). Fig. 20 (a, b, c) shows the EDS analysis image with the particle counts for run 6.

Table 17. Chemical compositions present at the recast layer, heat affected zone, and base metal for runs 6, 7, and 8

Run number	Elements	Recast Layer		Heat Affected Zone		Base Metal	
		Weight %	Atomic %	Weight %	Atomic %	Weight %	Atomic %
6	C K	4.04	8.45	3.83	15.44	4.46	17.68
	O K	37.26	58.54	0.93	2.82	0.79	2.34
	AlK	7.85	7.31	0.16	0.28	0.16	0.28
	TaM	0.14	0.02	0.22	0.06	0.39	0.10
	SiK	0.00	0.00	0.00	0.00	0.00	0.00
	CdL	0.34	0.08	0.31	0.13	0.41	0.17
	TiK	31.58	16.57	1.35	1.37	2.11	2.10
	CrK	17.37	8.40	20.20	18.82	19.81	18.16
	MnK	0.34	0.15	0.52	0.46	0.83	0.72
	FeK	0.54	0.25	18.96	16.44	19.08	16.28
	CoK	0.19	0.08	0.62	0.51	1.66	1.34
NiK	0.36	0.15	52.90	43.66	50.28	40.81	
7	C K	5.05	10.34	4.99	19.40	4.42	17.53
	O K	37.31	57.28	1.03	2.99	0.84	2.51
	AlK	9.35	8.51	0.31	0.54	0.28	0.50
	TaM	0.27	0.04	0.39	0.10	0.58	0.15
	SiK	0.00	0.00	0.00	0.00	0.00	0.00
	CdL	0.43	0.09	0.52	0.21	0.25	0.11
	TiK	34.52	17.70	1.56	1.52	1.58	1.57
	CrK	9.98	4.71	18.95	17.00	19.60	17.97
	MnK	0.82	0.37	1.13	0.96	1.06	0.92
	FeK	0.73	0.32	18.65	15.58	18.26	15.59
	CoK	0.46	0.19	1.44	1.14	1.55	1.25
NiK	1.08	0.45	51.04	40.56	51.58	41.90	
8	C K	9.89	19.42	5.99	22.64	3.63	14.69
	O K	37.49	55.26	1.06	3.01	0.92	2.80
	AlK	3.96	3.46	0.18	0.30	0.54	0.97
	TaM	1.70	0.22	0.64	0.16	0.35	0.09
	SiK	0.00	0.00	0.00	0.00	0.00	0.00
	CdL	0.39	0.08	0.44	0.18	0.42	0.18
	TiK	14.36	7.07	1.20	1.14	2.22	2.25
	CrK	29.17	13.23	18.46	16.12	20.08	18.76
	MnK	0.06	0.03	0.82	0.68	0.69	0.61
	FeK	1.95	0.82	18.19	14.78	17.96	15.63
	CoK	0.08	0.03	1.34	1.03	0.91	0.75
NiK	0.95	0.38	51.69	39.96	52.27	43.26	

The elemental composition of the Inconel alloy after being machined with various parameter settings yields an unexpected result of the atomic and weight percentages as indicated in summary Table 17. Even though Inconel is a nickel-based alloy, there is hardly any trace of Ni in the recast layer (Fig. 20 a). Just 0.36 weight percent and 0.15 atomic percent Ni are discovered at the recast layer for run number 6. Run 7 showed a 1.08 weight percentage and 0.45 atomic percentage of Ni at the recast layer. Likewise, 0.95 weight proportion and 0.38 atomic proportion of Ni are found at the recast layer after run 8.

Nevertheless, Ni is present in the heat-affected zone in the same amount as base metal as observed in all three runs. A similar finding was observed in the case of Fe. However, Ti and O are seen to be present in significant amounts at the recast layer (Fig. 20 a, showing high peaks for Ti and O). It is believed that oxygen atoms that were dissolved in distilled water during the quick cooling action were trapped at the recast layer. Oxygen may also be present as oxides formed during the bombardment process, as indicated earlier. However, the appearance of huge amounts of Ti in the recast layers is an interesting phenomenon. The copper electrode has 0.029% of Ti which might have contributed to the high amount of Ti in the recast layer. However, this phenomenon demands further study to be certain about the abnormally high presence of Ti in the recast layer. The amounts of other elements including Mn, Cr, Co, Cd, Ta, and C were the same as for the base metal. Another important development is that, while peak current and pulse on time for runs 6 and 8 were the same, material removal rate and surface roughness were found to be lower for lower peak current. There was no significantly detectable recast layer when the peak current was decreased. The Ni content increased from 0.15 atomic percent to 0.38 atomic percent and from 0.36 weight percent to 0.95 weight percent. In the area of the body impacted by heat, little cracks are seen. The recast layer thickness and disunity were raised while maintaining a middle-range peak current and increasing pulse on time.

5. Conclusion

The present research was conducted to investigate the influence of EDM parameters, such as peak current, Pulse on Time, and concentration of Nano-powder in distilled water-based dielectric on EDM response parameters – material removal rate (MRR), tool wear rate (TWR) and surface roughness (SR). The experimental investigations were conducted using the Response Surface Methodology approach. The results of the responses were developed in mathematical forms. To attain the best possible response values, RSM and GA response optimizations were employed. The following is a summary of the findings that were derived from the work:

- It was found that Peak Current, Powder Concentration and pulse on Time have a significant impact on surface roughness. A combination of Peak Current (17-20) Amp with Pulse on Time (270-350) μ s and Powder Concentration (1.50-2.25) g/L was found to result in lesser SR and an optimum range of MRR and TWR.
- Development of the models of the three responses using the response surface technique and optimizing them using RSM and GA has yielded a valuable procedure for determining optimized process parameters for the Nano PMED Process.
- Maximum Material Removal Rate 0.02336g/min is achieved from 48.5224 Amp peak current, 275 μ s pulse on time and 3.25 g/L powder concentration.
- Minimum Surface roughness of 4.361 μ m has been found from 15 Amp peak current, 150 μ s pulse on time and 5 g/L powder concentration which indicates the higher MWCNT concentration presents better surface finish.
- Minimum tool wear of 0.00085 g/min has been derived from 6.47759 Amp peak current, 275 μ s pulse on time and 3.25 g/L powder concentration which is a proof that lowest peak current combined with moderate pulse on time and powder concentration provides minimum surface roughness.
- The RSM optimization suggests that a Peak Current should be lower (19.925 Amp), Pulse on Time should be close to the maximum limit (307.967 μ s), and a

Powder Concentration should be at the lower limit of the range of 1.5 g/L, for optimum of MRR 0.012 g/min, TWR (0.001 g/min) and SR (5.098 μm).

- GA optimum suggested a Peak Current of 20.178 Amp, Pulse On-Time of 398.753 μs , and Powder Concentration of 3.66 g/L for the optimum value of MRR of 0.012 g/min, TWR of 0.003 g/min and SR of 5.229 μm . However, validation tests suggest that GA provides optimized values closer to the experimental values.
- EDS investigation of the machined surface reveals a significant transfer of C and Cu elements. Cu atoms migrate onto the machined surface more readily as a result of tool wear. The amount of carbon at the machined surface is also influenced by the presence of MWCNTs in the dielectric media. Carbon content increases with increasing MWCNT concentration.

References

- [1] Gong L, Su Y, Liu Y, Zhao W, Khan AM, Jamil M. Investigation on Machinability Characteristics of Inconel 718 Alloy in Cryogenic Machining Processes. *Lubricants*. 2023;11(2): 82. <https://doi.org/10.3390/lubricants11020082>
- [2] Vereschaka A, Milovich F, Andreev N, Migranov M, Alexandrov I, Muranov A, et al. Specific Application Features of Ti-TiN-(Ti,Cr,Al)N, Zr-ZrN-(Zr,Mo,Al)N, and ZrHf-(Zr,Hf)N-(Zr,Hf,Cr,Mo,Al)N Multilayered Nanocomposite Coatings in End Milling of the Inconel 718 Nickel-Chromium Alloy. *J Compos Sci*. 2022; 6(12): 382. <https://doi.org/10.3390/jcs6120382>
- [3] Smak K, Szablewski P, Legutko S, Krawczyk B, Miko E. Investigation of the Influence of Anti-Wear Coatings on the Surface Quality and Dimensional Accuracy during Finish Turning of the Inconel 718 Alloy. *Materials* (Basel). 2023;16(2) : 715. <https://doi.org/10.3390/ma16020715>
- [4] Zhao C, Zhao Y, Zhao D, Liu Q, Meng J, Cao C, et al. Modeling and Prediction of Water-Jet-Guided Laser Cutting Depth for Inconel 718 Material Using Response Surface Methodology. *Micromachines*. 2023;14(2) : 234. <https://doi.org/10.3390/mi14020234>
- [5] Sahu SK, Jadam T, Datta S, Nandi G. Effect of using SiC powder-added dielectric media during electro-discharge machining of Inconel 718 superalloys. *J Brazilian Soc Mech Sci Eng [Internet]*. 2018;40(7):1-19. <https://doi.org/10.1007/s40430-018-1257-7>
- [6] Lepcha LP, Dewan PR, Phipon R. Experimental investigation for surface roughness during electrical discharge machining process of super alloy inconel 718 using silicon powder mixed dielectric. *AIP Conf Proc*. 2020; 2273. <https://doi.org/10.1063/5.0024915>
- [7] Jawahar M, Sridhar Reddy C, Srinivas C. A review of performance optimization and current research in PMEDM. *Mater Today Proc*. 2019; 19:742-7. <https://doi.org/10.1016/j.matpr.2019.08.122>
- [8] Jadam T, Sahu SK, Datta S, Masanta M. Powder-mixed electro-discharge machining performance of Inconel 718: effect of concentration of multi-walled carbon nanotube added to the dielectric media. *Sadhana - Acad Proc Eng Sci*. 2020; 45: 135. <https://doi.org/10.1007/s12046-020-01378-2>
- [9] Abdul-Rani AM, Nanimina AM, Ginta TL, Rao TVVLN, Pedapati SR. Application of nano aluminum in modified EDM: pmedm. *ARPN J Eng Appl Sci*. 2016;11(20):12117-21.
- [10] Ahmad S, Lajis MA, Haq RHA, Arifin AMT, Rahman MNA, Haw HF, et al. Surface roughness and surface topography of Inconel 718 in powder mixed dielectric electrical discharge machining (PMEDM). *Int J Integr Eng*. 2018;10(5):181-6. <https://doi.org/10.30880/ijie.2018.10.05.027>

- [11] Deltombe R, Kubiak KJ, Bigerelle M. How to select the most relevant 3D roughness parameters of a surface. *Scanning*. 2014;36(1):150-60. <https://doi.org/10.1002/sca.21113>
- [12] Kabir H, Garg N. Rapid Prediction of Cementitious Initial Sorptivity via Surface Wettability. *npj Mater Degrad*. 2023; 7: 52. <https://doi.org/10.1038/s41529-023-00371-4>
- [13] Kumar A, Vivekananda K, Abhishek K. Experimental Investigation and Optimization of Process Parameter for Inconel 718 Using Wire Electrical Discharge Machining. *J Adv Manuf Syst*. 2019;18(3):339-62. <https://doi.org/10.1142/S0219686719500185>
- [14] Assarzadeh S, Ghoreishi M. A dual response surface-desirability approach to process modeling and optimization of Al2O3 powder-mixed electrical discharge machining (PMEDM) parameters. *Int J Adv Manuf Technol*. 2013;64(9-12):1459-77. <https://doi.org/10.1007/s00170-012-4115-2>
- [15] Anand A, Behera AK, Das SR. An overview on economic machining of hardened steels by hard turning and its process variables. *Manuf Rev*. 2019;6(4):1-9. <https://doi.org/10.1051/mfreview/2019002>
- [16] Wang J, Sun Z, Dai Y, Ma S. Parametric optimization design for supercritical CO2 power cycle using genetic algorithm and artificial neural network. *Appl Energy* [Internet]. 2010;87(4):1317-24. <https://doi.org/10.1016/j.apenergy.2009.07.017>
- [17] Stergioudi F, Prospathopoulos A, Farazas A, Tsirogiannis EC, Michailidis N. Mechanical Properties of AA2024 Aluminum/MWCNTs Nanocomposites Produced Using Different Powder Metallurgy Methods. *Metals (Basel)*. 2022;12(8) : 1315. <https://doi.org/10.3390/met12081315>
- [18] Sahu SK, Jadam T, Datta S. Performance of dielectric media (conventional EDM oil and distilled water) during machining of Inconel 825 super alloy. *Mater Today Proc* [Internet]. 2019;18:2679-87. <https://doi.org/10.1016/j.matpr.2019.07.129>
- [19] Audet C, Hare W. *Genetic Algorithms*. Springer Ser Oper Res Financ Eng. 2017;57-73. https://doi.org/10.1007/978-3-319-68913-5_4